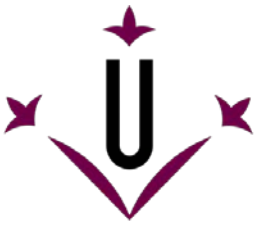

Modulating biopolymer electrical charge to optimize the assembly of edible multilayer nanofilms by the layer-by-layer technique

Alejandra Acevedo-Fani

Laura Salvia-Trujillo

Robert Soliva-Fortuny

Olga Martín-Belloso *

Department of Food Technology

University of Lleida – Agrotecnio Center

Av. Alcalde Rovira Roure 191

25198, Lleida, Spain

* Author to whom correspondence should be addressed: omartin@tecal.udl.es

ABSTRACT

The aim of this work was to study the influence of biopolymer (alginate-ALG; chitosan-CHI) charge on the formation of multilayer nanofilms by the layer-by-layer (LbL) technique. The electrical charge of ALG and CHI (*high*, *medium* or *low*) was modulated by adjusting the pH of biopolymer solutions. The amount of biopolymer deposited in multilayers depended on the charge of ALG and CHI solutions. The lower the charge the higher the deposition rate due to the higher number of biopolymer molecules needed to neutralize the previous layer. *Medium* and *low* charge biopolymers led to a drastic change in the wettability of multilayers, being ALG layers strongly hydrophilic and CHI layers strongly hydrophobic. The SZP alternatively changed from negative to positive using ALG or CHI. This effect was more pronounced using *highly* charged biopolymers. Results obtained in this study evidenced that the multilayers properties can be tuned by controlling the biopolymer electrical charge.

KEYWORDS: layer-by-layer, sodium alginate, chitosan, multilayers, electrostatic deposition

INTRODUCTION

Over the past few years, there has been a growing interest in nanotechnology as a versatile tool to design new types of materials. Multilayer nanofilms formed by the layer-by-layer (LbL) electrostatic deposition have been extensively used as a simple strategy to coat and functionalize the surface of materials with different applications in biomedicine, pharmacology and biomaterials science, among others. In the food sector, multilayer nanofilms offer a wide range of interesting applications such as thin edible coatings, functionalization of food packaging surfaces or encapsulation of food bioactive compounds with controlled release under certain conditions [1–3].

The LbL technique is based on the assembly of several thin layers by alternating the adsorption of oppositely charged polyelectrolytes on a charged substrate. The LbL process is mainly driven by electrostatic forces, although other interactions such as hydrogen bounding, hydrophobic and van der Waals forces may intervene [4]. Each deposited layer leads to a charge overcompensation that has two important consequences: i) the repulsion of equally charged molecules and thus self-regulation of the adsorption and restriction to a single layer and; ii) the formation of a new layer by the adsorption of oppositely charged molecules on the top of the previous layer [5]. This process results in the formation of multilayer nanofilms of 10-100 nm per layer, and the average thickness is determined by the number of layers of the film.

A variety of polysaccharides could be used to form edible multilayer nanofilms. Alginates are unbranched polysaccharides extracted from marine brown algae consisting of (1→4) linked β-D-mannuronic acid and α-L-guluronic acid residues. In aqueous solutions, alginates behave as polyanions (pKa ≈ 3.6) due to the presence of -COOH groups along the molecular chains that can be deprotonated to confer negative charges [6]. Chitosan is a copolymer naturally abundant in the exoskeleton of crustaceans,

fungal cell walls and in other biological materials. It is mainly composed by β-(1-4)-2-acetamido-D-glucose and β-(1-4)-2-amino-D-glucose units and it is generally described in terms of degree of deacetylation. Chitosan acts as a cationic biopolymer (pKa ≈ 6.2) in acidic conditions due to the protonation of -NH_2 groups in the chemical structure. The formation of stable complexes between alginate and chitosan through electrostatic interactions has been described by other authors [7,8].

In spite of the simplicity of the LbL technique, processing parameters such as coating material concentration, washing and drying steps, ion concentration, and pH of solutions may influence the adsorption kinetics of the films [4,9]. The solution pH is an important factor to be considered since its variation alters the dissociation of charged polysaccharides and thereby, the magnitude of the electrical charge. This fact directly affects the electrostatic interactions between polysaccharides, changing the adsorption process and the film properties. The assembly of alginate and chitosan through the layer-by-layer technique has been previously described for biomedical approaches [10–12]. However, scarce systematic studies have reported the effect of the electrical charge of both biopolymers modulated by pH for food purposes. The study of the deposition during the LbL process is crucial to understand the assembly mechanism and optimize the conditions for the use of nanofilms in practical applications. The objective of this work was to obtain multilayer nanofilms based on natural polymers such as alginate and chitosan and evaluate the effect of the electrical charge of the biopolymers solutions on the formation and film properties of multilayers through the layer-by-layer assembly method.

MATERIALS AND METHODS

MATERIALS

Quartz slides (suprasil® 300) were purchased from Hellma analytics (Müllhein, Germany) and polyethylene terephthalate (PET) sheets were obtained from Isovolta (Barcelona, Spain). Reactives for substrate aminolization such as, 3-aminopropyltriethoxysilane (APTS, 99 %), N,N-Dimethylformamide (DMF, 99,8 %) and 1,6-Hexanediamine (99,5 %) were purchased from Acros Organics (Geel, Belgium). Piperidine (99 %) was purchased from Sigma-Aldrich (Madrid, Spain). Methanol and bromophenol blue (BPB) were obtained from Fisher Scientific (Loughborough, UK). Ethanol Absolute and 1-propanol were purchased from Scharlau (Barcelona, Spain). Hydroclorhidric acid (HCl, 35-38%) was purchased from POCH (Gliwice, Poland). Chitosan (CHI, high molecular weight, deacetylation degree >75%) and sodium alginate (ALG; manucol® DH) were purchased from Sigma-Aldrich (Madrid, Spain) and FMC biopolymers (Scotland, UK), respectively. The pH of the polysaccharide solutions was adjusted with lactic acid (88-90%) and sodium hydroxide (NaOH) purchased from Scharlau (Barcelona, Spain). Deionized water (18,2 mΩ, Milli-Q ultrapure water system, Millipore) was used in all film-forming solutions and washing steps for the nanofilms fabrication.

SUBSTRATES PRE-TREATMENT

Quartz slides were cleaned with a Hellmanex® solution 2% (v/v) for 2 hours. Substrates were immersed in APTS (1% v/v) at 25 ºC during 30 minutes to induce a positive charge on the quartz surface, and rinsed with copious deionized water in order to remove reactive excess [13]. Quartz slides were left in a desiccator containing silica gel until nanofilms were assembled.

PET sheets were functionalized according to a method described by ref [14] with some modifications. PET rectangles (6 cm x 2 cm) were cleaned in propanol/water 1:1 solution during 3 hours. Briefly, the sheets were submerged in tubes containing 10 mL

of 1,6-hexanediamine/methanol solution (1 M) at 50 ºC during 4 hours to induce the aminolysis reaction, giving a positive charge to the PET surface. PET substrates were removed from the tubes and washed with methanol, and then dried in vacuum at room temperature (25 ºC) for 12 hours. The PET sheets were treated with HCl 0,1 M during 3 hours at 25ºC to protonate amine groups attached to the material surface. After this process the rectangles were left in vacuum for at least 12 hours and 25ºC.

POLYELECTROLYTE SOLUTION PREPARATION

Sodium alginate and chitosan solutions were prepared at a concentration of 0.5 % w/w. Sodium alginate was dissolved in ultrapure water and chitosan was prepared in lactic acid solution (1 % v/v) to promote protonation of amino groups in the biopolymer molecule and therefore increase its solubility. Polysaccharide solutions were left under agitation during 5 hours. Alginate and chitosan solutions with different electrical charges (*high, medium* and *low*) were prepared by adjusting the pH of the solutions using lactic acid or NaOH solutions (Table 1).

ZETA POTENTIAL

The electrical charge of ALG and CHI solutions was evaluated by phase-analysis light scattering using a laser diffractometer (Zetasizer NanoZS, (Malvern Instruments Ltd, UK).

LAYER-BY-LAYER ASSEMBLY

Nanofilms were assembled on two types of substrates. Quartz slides were used to obtain the UV-visible spectra and PET rectangles were used for the other determinations. The previously cleaned and positively charged substrates were submerged in alginate solutions in order to form the first layer. Substrates remained in this solution during 20 min. After the adsorption process, samples were rinsed twice in ultrapure water at the same pH of alginate solutions for 5 min. This step was necessary

to remove the sodium alginate molecules that were not bound to the substrate. Straightaway, substrates were immersed in chitosan solutions for 20 min to obtain the second layer. In this step, the positively charged chitosan molecules were adsorbed to the previous negatively charged alginate layer by means of electrostatic interactions. After this, the process was followed by two rinse steps with ultrapure water at the pH of chitosan solutions for 5 min. Alternate deposition of layers was repeated to obtain a multilayered structure film. For the purpose of this work, 10 layers were considered as a reasonable number to study the buildup process and the differences in film architecture according to the pH used during the assembly. When the deposition of layer was complete the nanofilms were dried using a nitrogen gas flow.

CHARACTERIZATION OF SUBSTRATES

Determination of the concentration of amine groups

After the aminolysis reaction, the concentration of amine groups introduced to the PET sheets and quartz slides were analyzed with a method previously reported by ref [15]. The substrates were immersed in 25 mL of BPB/DMF solution (0,1 mg/mL) for 30 minutes. Then rectangles were removed from the previous solution and washed with copious ethanol to remove unbounded dye. PET sheets were treated with 10 ml of piperidine/DMF solution (20 %), and the absorbance of the solution obtained was measured at λ = 605 nm. The surface concentration of amine groups was calculated from Lambert's-Beer law following equation 1:

$$A = \varepsilon . l . c \quad (1)$$

Where A is the absorbance of the sample, ε is the molar extinction coefficient (BPBε_{605} = 91,800 L.mol^{-1}.cm^{-1}), l is the path length (1 cm) and c is the sample concentration. The concentration of amine groups found in untreated PET and quartz slides was 0.04 ± 0.01 nmol/cm^2, and after being treated, final concentrations increased

up to 0.63 nmol/cm^2 and 0.11 ± 0.01, respectively (figure 1). In both cases it could be confirmed that –NH_2 groups were incorporated onto the substrates.

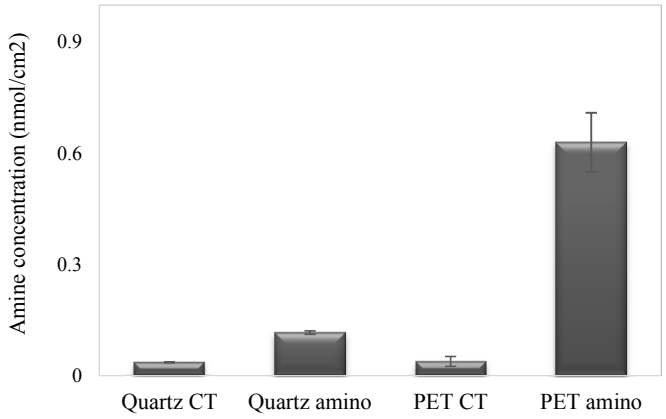

Figure 1. Surface concentration of amine groups on untreated PET or quartz substrates (PET CT and Quartz CT) and after aminolization (PET amino and Quartz amino).

CHARACTERIZATION OF EDIBLE NANOFILMS

Spectrophotometric measurements

The layer-by-layer assembly of ALG and CHI on quartz slides was monitored using a UV-visible-NIR spectrometer (V-670, Jasco Corporation, Tokio, Japan). The absorption spectra of bilayers were obtained. The absorbance of ALG in aqueous solutions is increased as a function of the biopolymer concentration (Figure 2A). ALG (0.5%) presented a bell-shaped absorption peak at 200 nm, whereas CHI does not show appreciable absorbance at that wavelength range (Figure 2B), thus multilayer deposition was assessed using 200 nm.

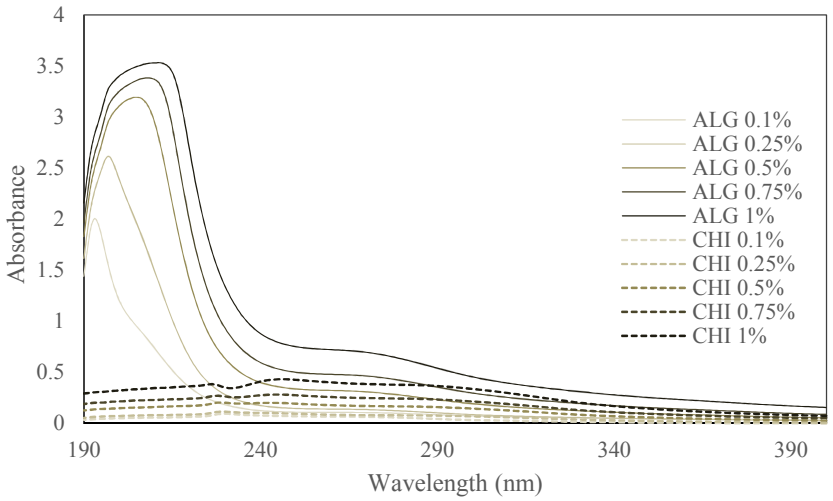

Figure 2. (A) Absorption spectra of ALG and CHI in aqueous phase at different concentrations (0.1 – 1 %).

Surface ζ-potential analysis

The ζ-potential is an important and useful indicator of the electrical charge at the film surface. The zeta potential of nanofilms after each deposition of layers was determined using the Zetasizer NanoZS laser diffractometer, (Malvern Instruments Ltd, Worcestershire, UK) equipped with a surface ζ-potential cell unit (ZEN1020), specially designed for zeta potential analysis in flat surfaces. Nanofilms formed on PET and attached to a sample holder were placed between two electrodes of the surface ζ-potential cell. After that, samples were immersed in an appropriated aqueous solution containing tracer particles. The negative and positive particles were polystyrene latex particles in buffer solution pH 9 (DTS1235, Malvern instruments) and quaternary ammonium salts in solution (obtained from fragrance-free fabric conditioner), respectively. The electrical charge of these tracer particles was opposite to the charge of the surface to be analyzed. The tracer ζ-potential was measured by phase-analysis light scattering (PALS) at 5 distances from the sample surface. By plotting the zeta potential

as a function of displacement from the surface, the software equipment extrapolated this relationship to zero displacement to obtain the surface ζ-potential of nanofilms.

Water contact angle measurements

The contact angle of the nanofilms after each layer deposition was determined using a DSA25 Krüss goniometer (Krüss GmbH, Hamburg, Germany) equipped with an image analysis software (Drop Shape Analysis System, Krüss GmbH, Germany). By applying the sessile drop method, five deionized water drops of 1 μL were created at the tip of the syringe and carefully placed along the PET sheet covered with nanofilms. Measurements were conducted immediately after drop deposition and tests were carried out at room temperature. The contact angle was calculated using the Young-Laplace fit.

SEM imaging

SEM imaging measurements were performed using a J-6510 scanning electron microscope (JEOL Ltd, Tokio, Japan). Aluminum stubs containing PET covered with nanofilms were treated with carbon and metalized with evaporated gold, using a SCD 050 sputter coater (Balzers Union AG, Liechtenstein). This step was necessary to confer electrical conductive properties to the substrate with nanofilms. Samples were analyzed with an acceleration voltage of 5 kV.

Thermal properties

The thermal properties of ALG and CHI nanofilms fabricated on PET substrates were determined using a differential scanning calorimeter (DSC822e, Mettler Toledo S.A.E., Barcelona, Spain). Samples were heated from 0 ºC to 400 ºC at a rate of 10 ºC/min under an atmosphere of inert nitrogen. The glass transition temperature (T_g), the melting temperature (T_m) and the enthalphy of melting (ΔH_m) were reported from the thermograms. The melting curve was integrated using StartE v.11 software (Mettler Toledo S. A. E., Barcelona, Spain), in order to obtain the enthalpy of melting.

Statistics

Experiments were repeated twice and samples were analyzed by triplicate. The average and standard deviations of data were presented. ANOVA analysis was performed using Statgraphics plus 5.1 software (Statistical Graphics Co., Rockville, MD, EE.UU) and differences among average results were assessed using Fisher's least significant difference (LSD) method with a significance level of 95 %.

RESULTS AND DISCUSION

EFFECT OF THE BIOPOLYMER CHARGE ON THE BUILDUP

The pH of the biopolymer solution determines the ionization of the surface groups on a macromolecule and therefore the final surface charge density[17]. ALG and CHI are weak polyelectrolytes, thus the degree of dissociation of their functional groups, and in turn, the electrical charge can be controlled by changing the pH of the solutions. In this study, three combined pH settings for ALG and CHI were selected in order to obtain polysaccharide solutions with a *low*, *medium* and *high* electrical charge during the formation of multilayers. Table 1 shows the electrical charge expressed by ζ-potential of ALG and CHI solutions at different pH conditions corresponding to three different levels of charge. In the case of ALG, the ζ-potential values of *high*, *medium* and *low* charge polysaccharides used for the formation of nanofilms were -87.4 mV, -77.3 mV and -41.3 mV at pH 7, 5 and 3, respectively. Similarly, the ζ-potential of *high*, *medium* and *low* charge CHI chains in aqueous solutions were 77 mV, 68 mV and 27 mV at pH 3, 4 and 7, respectively. The change in the degree of ionization of both biopolymers can be explained by the protonation or deprotonation of the charged moieties, such as –COOH and $-NH_2$, under the presence of different concentrations of H^+ and OH^- ions in the surrounding media.

Table 1. Electrical properties of biopolymer solutions at different pH conditions.

Levels of electrical charge	Polysaccharide – pH	ζ-potential (mV)
High	ALG – 7	-87.4 ± 2.1
	CHI – 3	77.0 ± 4.0
Medium	ALG – 5	-77.3 ± 1.4
	CHI – 4	68.0 ± 4.0
Low	ALG – 3	-41.4 ± 1.6
	ALG - 7	27.0 ± 4.0

Results are presented as the average ± standard deviation. ALG: alginate solutions, and CHI: chitosan solutions.

To study the effect of the biopolymer electrical charge on the buildup of multilayers, absorbance spectra in the UV-visible range were obtained (Figure 3). Absorbance is, in principle, directly proportional to the amount of material deposited on the substrate after the formation of multilayers. The spectra of $(ALG\text{-}CHI)_{10}$ multilayer nanofilms showed absorbance around 200 nm, although, there is not a bell-shape peak at this absorbance, probably due to the formation of molecular complexes between ALG and CHI during the LbL procedure that could have influenced the optical properties. In fact, it is known that layers of oppositely charged polyelectrolytes form molecular *blends* that might present an intermediate molecular spectrum[17].

The absorbance increased as a function of the number of layers, regardless of the electrical charge of the polysaccharides chains (Figure 3A, 3B, 3C). This fact evidenced the deposition of material onto the substrate, thus confirming the effective buildup of nanolayers with the LbL technique by oppositely charged biopolymers. Nevertheless, the electrical charge of polysaccharides significantly affected the amount of material deposited in nanofilms. When multilayers were assembled with *low* charge ALG and CHI chains, the absorbance was significantly higher after each layer formation compared to the multilayers formed from *medium* or *high* charged biopolymers (Figure 3D). After 10-layers, nanofilms assembled with *high*, *medium* and *low* charge ALG and CHI chains exhibited significant differences in absorbance values, being of 0.2690 ±

0.016, 1.3 ± 0.4 and 1.55 ± 0.05, respectively. The differences observed in the absorbance of multilayer nanofilms depending on the electrical charge of the polysaccharide might be due to the different molecular conformations of the biopolymers under pH conditions selected. ALG presented a high electrical charge at pH 7 whereas CHI presented a high charge at pH 3. At these pH conditions, carboxylic groups of ALG and amino groups of CHI had a strong intra molecular repulsion exhibiting a well-extended molecular conformation. When the net charge is rather *high*, less amount of material is required to overcompensate surface charge during the adsorption process. On the contrary, when ALG and CHI have relatively *low* charge, at pH 3 and 7 respectively, most of the carboxylic groups of ALG and amino groups of CHI become neutral and the molecules tend to fold adopting loopy conformations. In consequence, greater amounts of material are required to achieve the charge reversal during the assembly process, thus increasing absorbance. In fact, this is what is typically observed when the multilayers assemblies are carried out with weak polyelectrolytes at different pH conditions [18,19]. For poly(allylamine hydrochloride) and poly(acrylic) acid multilayers, the film thickness dramatically decreases when the pH is between 6.5-7.5, and both polyelectrolytes are fully charged. However, if one of the two polyelectrolytes is partially charged at certain pH the film thickness is increased. Moreover, Pargaonkar et al.,[20] and Ai et al.,[21] observed that the thickness of multilayers made of poly(dimethyldiallyl ammonium chloride), sodium poly(styrenesulfonate) and gelatin on drug particles increased when gelatin in acidic pH was incorporated, and that behavior was attributed to changes in its molecular conformation. Other authors have described that thickness of the adsorbing layer can be modulated by changing the pH of the polyelectrolyte solution[11].

Additionally, the growth rate of nanofilms was evaluated (Figure 3D). Multilayers assembled with *high* charge polysaccharides exhibited a linear trend, meaning that absorbance at 200 nm increased uniformly in each bilayer. Conversely, multilayers formed from *medium* and *low* charge polysaccharides exhibited an exponential growth trend, which is characterized by an increasing rate of mass deposition for each additional layer with the number of layer depositions. A polyanion/polycation system that grows exponentially under certain conditions can also grow linearly when deposition conditions are modified [22]. A linear growth indicates that charged molecules in the solution interact exclusively with the outer layer of the multilayer film. However, when exponential growth occurs one of the polyelectrolytes is able to diffuse within the film structure toward the outer layer, and these free chains can interact with the adsorbing solution contributing to the film growth [23]. Therefore the results observed in the present work are in agreement with other studies, confirming that the charge density of the polysaccharide solution plays a key role in their capacity to form multilayers by the LbL technique [24]. Furthermore, changes in the growth type as a function of pH have been observed in multilayers made with polymers that behave as weak polyelectrolytes[25].

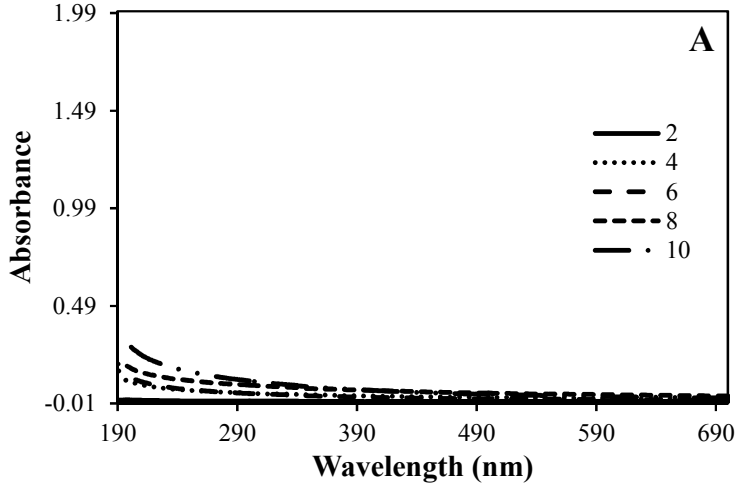

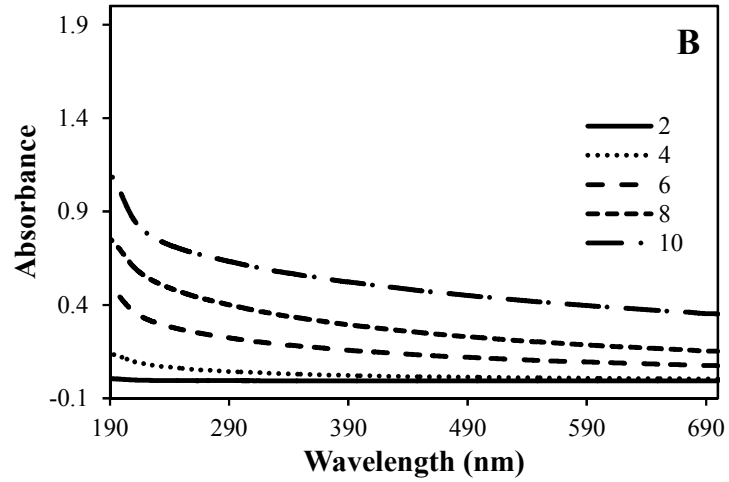

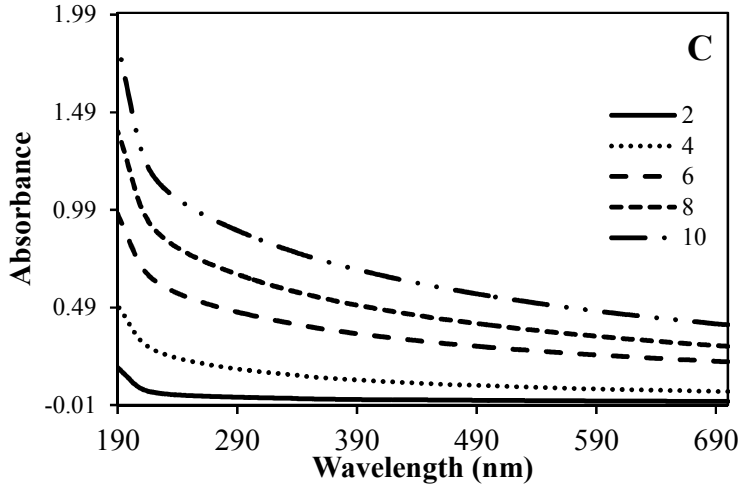

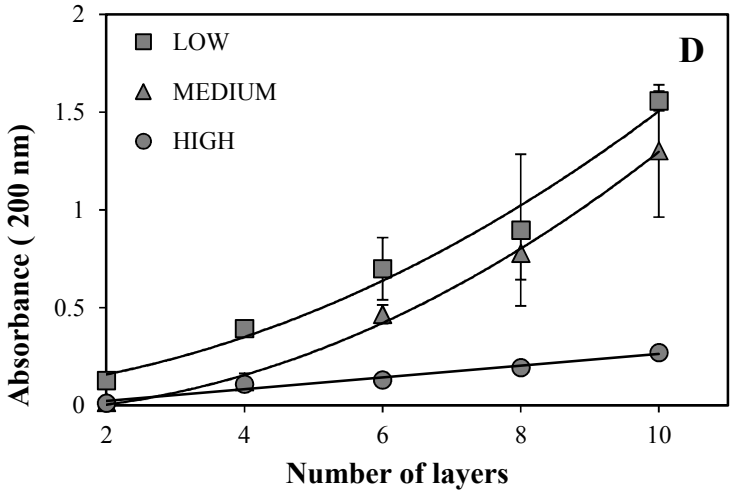

Figure 3. UV-visible spectra of sequential adsorptions of bilayers (2, 4, 6, 8 or 10 layers) at (A) *low*, (B) *medium* and (C) *high* electrical charge, according to table 1. (D) Absorbance at 200 nm of nanofilms as a function of the number of layers.

3.2. EFFECT OF THE BIOPOLYMER CHARGE ON THE SURFACE ζ-POTENTIAL

An important property of multilayers formed by electrostatic interactions is the ζ-potential, which is defined as the potential at the hydrodynamic slipping plane adjacent to the boundary phase [26]. To assess the effect of the polysaccharide charge on the electrical properties of nanofilms, the surface ζ-potential (SZP) was measured after each layer deposition (Figure 4). Initially, the aminolyzed PET was positively charged (49 ± 7 mV). After the first layer formation, the charge magnitude switched to negative in assemblies formed with *high* and *medium* charge ALG chains, suggesting that surface was completely saturated by the adsorbing molecules. Nevertheless, the first layer formed from low charge ALG chains did not show a change in SZP sign, although the magnitude decreased down to 5.0 ± 2.4 mV, which can be associated with a sparse coverage of the substrate. In this case, the positive SZP value may result from contributions of the low residual charge of ALG chains and the PET surface. Literature reports that a minimum charge density is required for the formation of multilayers and below this threshold, the charge reversal is not sufficient to achieve charge overcompensation [4,9]. However, despite the low charge of the first ALG layer, the results evidence that the formation of multilayers is possible and even presents an increased deposition when using low charge biopolymers as discussed earlier. In this line, the electrostatic interactions were not necessarily the main driving force responsible for the multilayers formation. The non-Coulombic interactions such as hydrogen bonding between neutral molecules, van der Waals forces or steric interactions, play an important role on the process of adsorption of multilayers. The impact of non-electrostatic interactions on the deposition of multilayer systems of cellulose and chitosan have been recently described in detail by other authors[27].

Moreover, the formation of multilayers from low charge polyelectrolytes have been reported, attributing this fact to the presence of synergistic non-electrostatic interactions that contribute to the layer formation [28,29]. After the consecutive addition of new layers of the oppositely charged biopolymers, the SZP of the subsequent layer presented a positive charge (CHI layers) or negative charge (ALG layers). This supports the fact that each layer adsorption leads to a charge reversal, providing a new opposite charge required to continue further adsorption steps. These results are consistent with the ζ-potential measured by Richert et al.,[30] on biopolymer-based (hyaluronan/chitosan) multilayers and by Ladam et al.,[31] on synthetic polymer-based (poly(allylamine hydrochloride)/ poly(sodium 4-styrenesulfonate)) multilayers, deposited on flat surfaces and determined by streaming potential measurements.

The charge of the biopolymer solution significantly affected the SZP of the successive layers formed. When *high* and *low* charge ALG and CHI solutions were used, the ALG layers (odd) and CHI layers (even) showed significantly more negative or more positive SZP, respectively, at increasing number of layers. However, this pattern was not observed for the *medium* charge biopolymer solutions, where the SZP of increasing number of ALG or CHI layers was significantly lower ($p<0.05$). These results are in concordance with those previously discussed in this work. The layers formed with *high* charge polysaccharides may present a greater number of ionizable groups on the surface that can increase the magnitude of electrical charge. In the case of layers formed with *low* charge polysaccharides the high surface charge may be attributed to the greater amount of polysaccharides chains needed to form the nanolayers that in turn, increase the number of charged groups on the surface. In all the assemblies the charge magnitude of even layers was greater than the charge magnitude of the odd layers suggesting a higher contribution of CHI to the electrical properties of nanofilms. The pH of solutions

containing biopolymers with ionizable groups could lead to irregular behaviors on the charge reversal during the LbL deposition. According to Zhang et al.,[32], the multilayers composed by hyaluronic acid and collagen followed a similar trend regarding the SZP. However, the magnitude of SZP remained relatively constant from the 8th layer at the different levels of charge, suggesting the stability of the system after the deposition of a certain amount of layers.

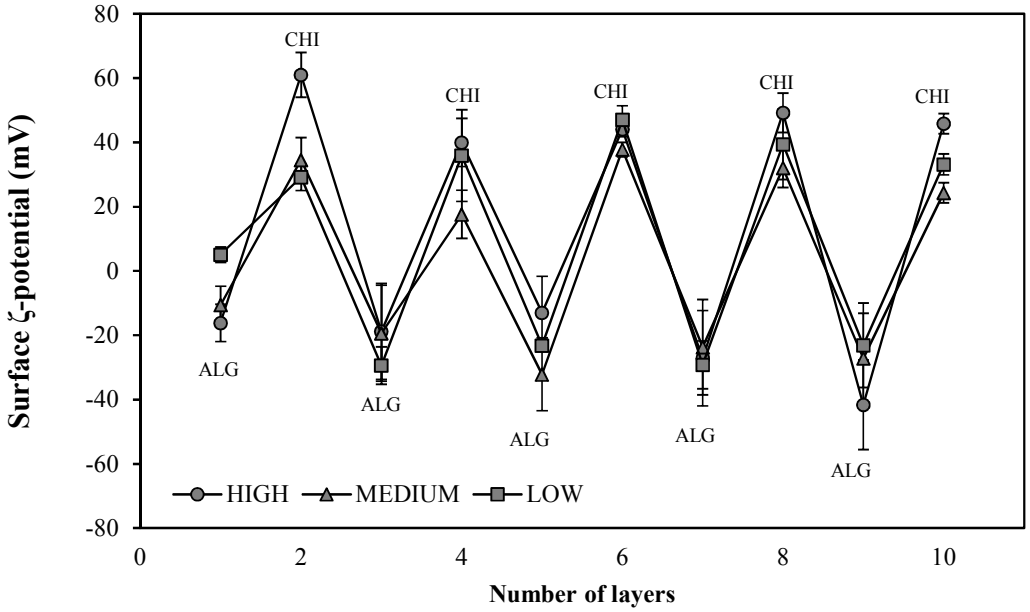

Figure 4. Surface ζ-potential (SZP) of multilayer nanofilms assembled from alginate (ALG) and chitosan (CHI) at *high*, *medium* and *low* electrical charge (according to table 1).

3.3. EFFECT OF BIOPOLYMER CHARGE ON THE CONTACT ANGLE

The contact angle is often used to describe the wetting behavior of films. It is defined as the angle formed at the intersection of the liquid, gas and solid phases [33]. There is a balance between the cohesion forces within a liquid and adhesion of a liquid to a solid[34]. The contact angle that creates a drop of water on the surface of the multilayers provides meaningful information to describe the hydrophilic or hydrophobic behavior of the nanofilm. The greater the contact angle value the more hydrophobic the film surface.

Figure 5 shows the contact angles of the multilayers assembled from biopolymers with different electrical charge. Water contact angles showed a zigzag trend when nanofilms passed from ALG-ending layers to CHI-ending layers with *low* and *medium* charge, indicating a pronounced change in the wetting properties of the multilayers. CHI layers were more hydrophobic, whereas ALG layers presented a strong hydrophilic behavior. This effect was more pronounce in multilayers formed with *low* charge biopolymers. Results are in good agreement with those found by other authors[35,36]. Conversely, no remarkable differences were observed in the results obtained from multilayers assembled with *high* charge polysaccharides ($p<0.05$), which could be correlated with the results of absorbance previously discussed (Figure 3). This means that the strong hydrophobic/hydrophilic interactions observed in multilayers made of *medium* and *low* charge biopolymers can be due to a greater amount of material deposited in each layer during the assembly process, originating more uniform and structured layers. On the contrary, the assemblies obtained from *high* charge polysaccharides did not show differences in the wetting properties during the sequential formation of new layers and presented the lower mass adsorption rate as well. This behavior suggests that the hydrophilic or hydrophobic character of the nanofilms is highly dependent on the experimental conditions used during the assembly of multilayers. For instance, Fu et al.,[37] have reported the strong effect of the film thickness on the wettability of multilayers made of two natural polyelectrolytes (heparin and chitosan). In thinner layers, the oppositely charged polysaccharides establish strong interactions originating well-interpenetrated structures in which the surface properties will be governed by the properties of the polysaccharide *blend* resulting in a less stratified multilayer structure. In thicker layers, the surface composition is rich in the last polysaccharide adsorbed and the chain segments of the outermost layer dominate the film wetting properties [31,38].

Thus, water contact angles observed in this study are strongly related with the differences in the amount of polyanion/polycation mass adsorbed during the LbL procedures. Other factors including the microstructure of multilayers might have an influence on the wettability. For example, in the work of Deng et al.,[39] the notable decrease in water contact angles of star-shaped supramolecule-deposited surface regarding to pristine polymeric surface coated by multilayers was attributed to a greater porosity of the first-mentioned surface, thus increasing its hydrophilicity.

On the other hand, contact angles of the outermost layers (CHI) increased as the electrical charge decreased, indicating an increase in surface hydrophobicity. Similarly, when the outermost layer was ALG significant differences were observed among assemblies at *low*, *medium* or *high* electrical charge ($p<0.05$). Contact angles tended to decrease as the polysaccharide electrical charge decreased, indicating that film surface increased their water affinity. These results indicate that the outermost layer and the thickness of the individual layers govern the wettability of multilayer nanofilms. This has important implications in the food sector, since multilayer nanofilms can be designed to provide strong hydrophobic properties in the case of dry food products sensitive to moisture effects, whereas hydrophilic multilayers can be used in products that need certain water activity to maintain their freshness.

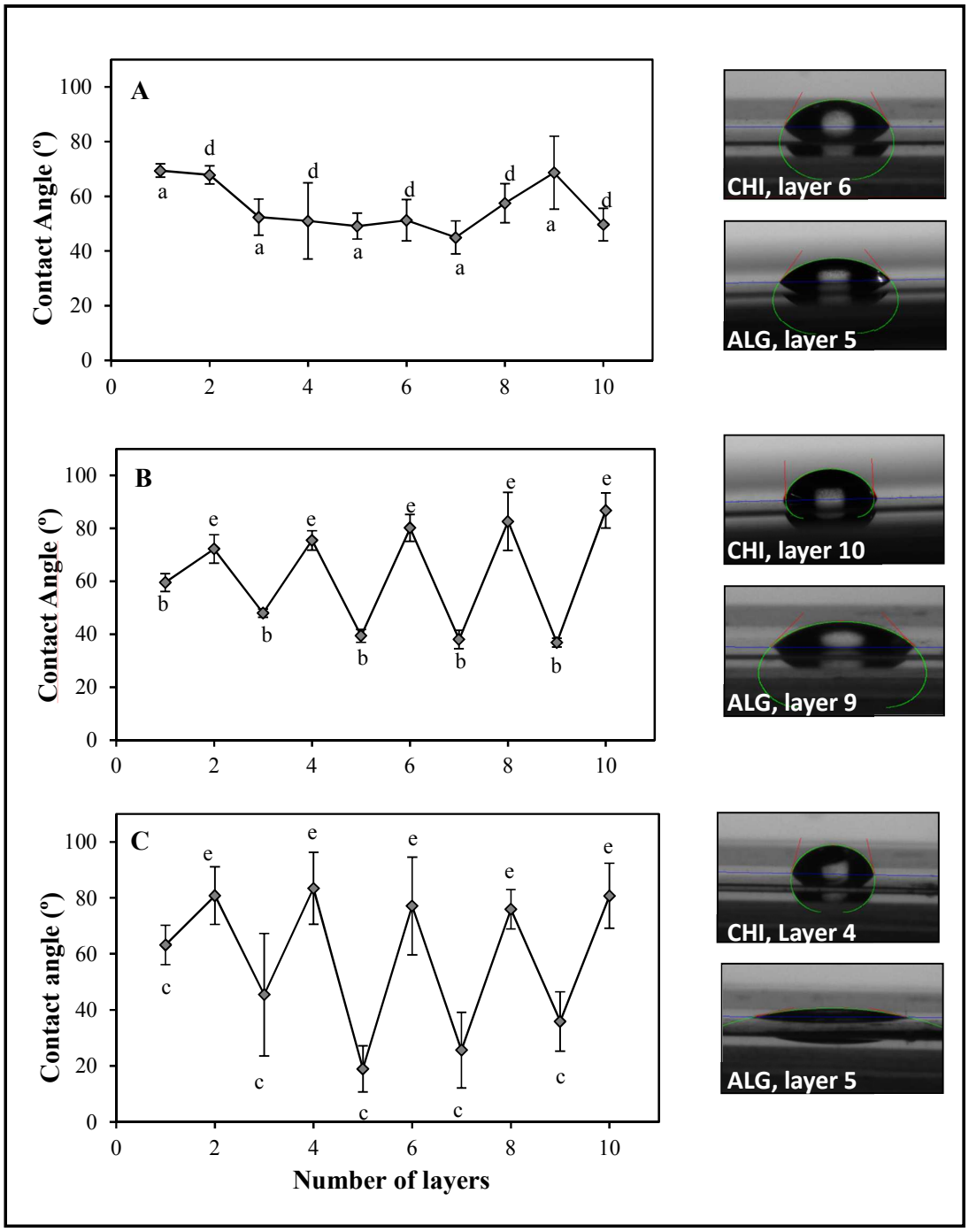

Figure 5. Water contact angle of multilayer nanofilms assembled from polysaccharides with different electrical charge; A) *low*, B) *medium* and C) *high*, according to table 1. Different letters means significant differences between layers ($p < 0.05$).

3.4. MICROSTRUCTURE

To study the film microstructure, multilayers fabricated from polysaccharides with *medium* electrical charge were selected, since the most uniform deposition was observed based on previous analyses of absorbance, SZP and contact angles. Figure 6A shows the uncoated PET substrate, where the surface present a smooth appearance. However, the micrographs taken after the coating PET with 10 layers reveal the presence of a thin film, thus confirming the formation of multilayers by the layer-by-layer method. According to the image 6B, multilayer nanofilms present film thickness of 297 nm in ten layers. The structure shows an appreciably grainy appearance. Additionally, the cross section of nanofilms (figure 6C) reveals that layers present a solid structure, but it is not possible to distinguish a nanolayered structure. The topography of the 10-layer nanofilm was also evaluated (Figure 6D). The film surface was characterized by the presence of small clusters with a globule-like appearance connected between them, probably due to formation of polyelectrolyte complexes of ALG/CHI onto the surface during the LbL assembly process [8].

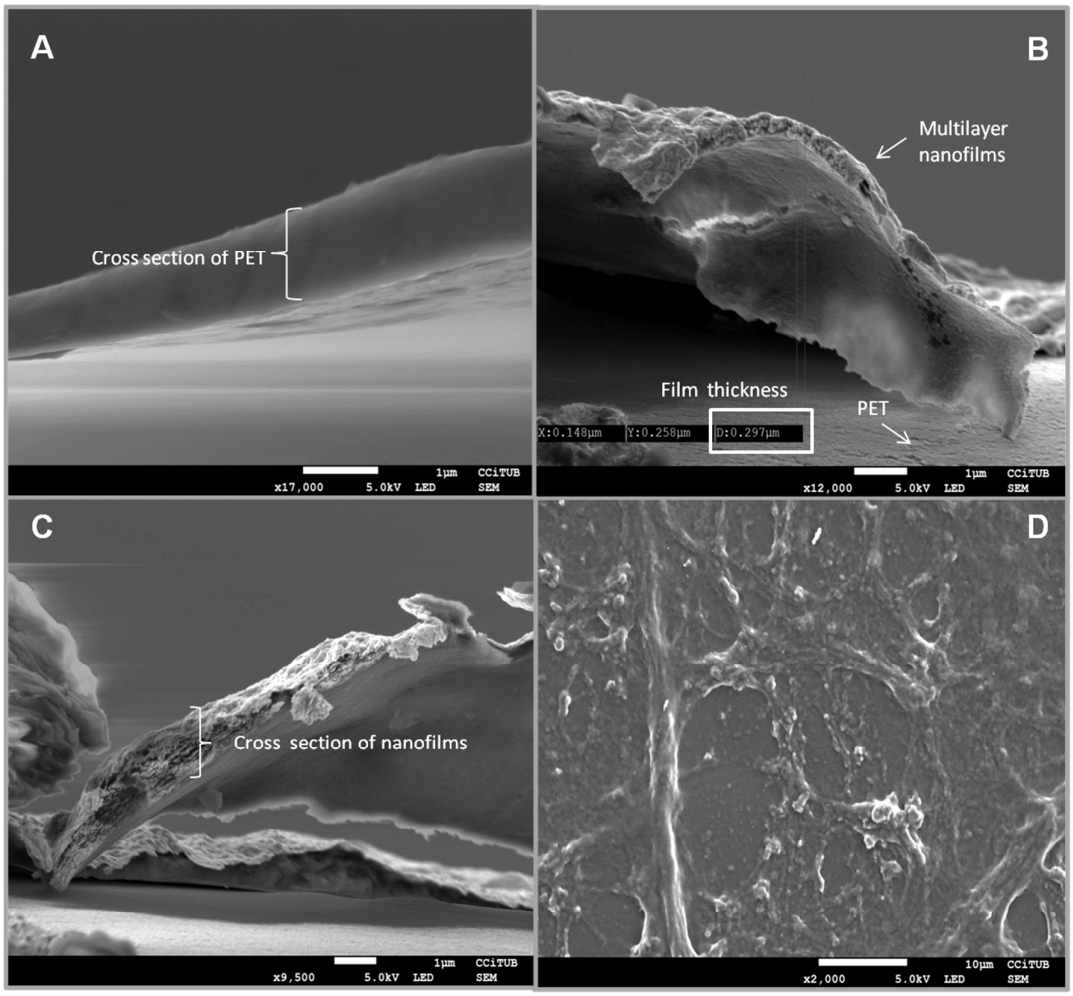

Figure 6. SEM images obtained from multilayers formed from ALG and CHI solutions at *medium* electrical charge. (A) Cross-sectional view of PET without coating. (B) 10-layer nanofilms formed onto PET, film thickness = 297 nm. (C) Cross section of multilayer nanofilms. (D) The topography of films at x2000.

3.5. THERMAL PROPERTIES

Thermal properties were evaluated in assemblies formed with *medium* charge polysaccharides considering the same criteria used for SEM analyses. Thermograms of uncoated and coated PET containing 10-layer nanofilms are presented in Figure 7. The thermal profile of PET coated by the alginate and chitosan multilayers showed a similar behavior regarding to uncoated PET. The glass transition temperature (T_g) and melting temperature (T_m) were 78 ºC and 257 ºC; whereas the T_g and T_m found for uncoated

PET was 78 ºC and 255 ºC, respectively. The latter results of uncoated PET are in good agreement with those reported by other authors [40–42]. The presence of multilayers on the PET film did not significantly affect the T_g and T_m obtained in the DSC analysis, probably due to differences in the mass ratio between the PET film and multilayer nanofilms, predominating the PET thermal properties. The glass transition temperature is reversible and occurs when an amorphous material is heated or cooled in a certain temperature range. Furthermore, the melting temperature is the point where the material changes from solid to liquid phase due to an increase in molecular mobility[43]. These thermal properties are especially relevant from a practical point of view in materials coated with biopolymer-based multilayers because they greatly determine the mechanical behavior of the material.

Moreover, the melting enthalpy (ΔH_m) of coated PET with multilayers slightly increased compared to the melting enthalpy of uncoated PET. This could be related to the ability of multilayers of acting as barrier to the diffusion of gases originated by the thermal degradation process, from the bulk to the surface of the film, contributing to slow down the polymer degradation[44]. In addition, the surface modification by the carboxylic groups and amino groups from CHI and ALG, or an increase in the polymer crystallinity may have a contribution to the enthalpy changes, as it was previously discussed in the thermal properties of PET coated with five multilayers of alginate and chitosan[45].

Sample	T_g (ºC)	T_m (ºC)	ΔH_m (J/g)
PET	78 ± 0.5	255 ± 1	45 ± 2
PET + nanofilms	78 ± 0.5	257 ± 2	49 ± 1

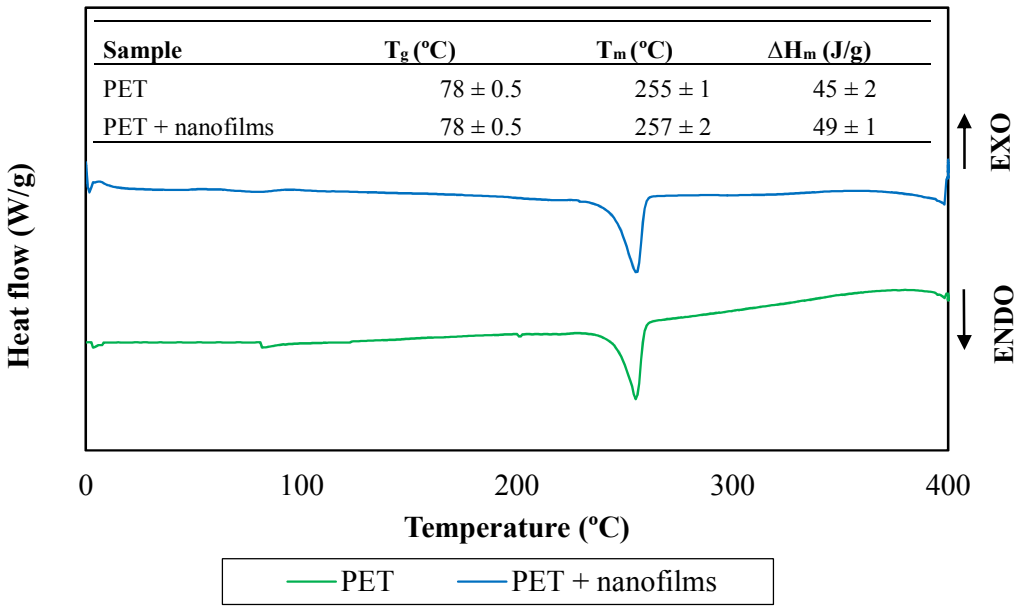

Figure 7. DSC thermograms and thermal properties of PET uncoated and PET coated with $(ALG\text{-}CHI)_{10}$ multilayer nanofilms formed from *medium* charged biopolymers, according to table 1.

3.6. CONCLUSIONS

The effect of the electrical charge of ALG and CHI on the formation of multilayer nanofilms was investigated. A linear growth type was characteristic of nanofilms assembled from highly charged ALG and CHI layers, however, as the polysaccharides charge diminished nanofilms exhibited an exponential growth type, which was associated to the different electrostatic and non-electrostratic interactions between polysaccharides under the pH conditions selected in this study. The amount of material adsorbed substantially increased when *low* charge polysaccharides were used, and conversely, mass adsorption was lower when the polysaccharides were fully charged. SZP of multilayers switched from negative (in ALG layers) to positive (in CHI layers) confirming the LbL deposition. Differences in SZP with regard to the charge of polysaccharides were also found. Wetting properties were affected by the electrical charge of ALG and CHI. A correlation between the water contact angles and the amount

of material absorbed was observed. From these results it can be conclude that the buildup of multilayers can be easily modulated by controlling the electrical charge of the oppositely charged polysaccharides to reach specific properties. In addition, this study provides valuable knowledge for the rational selection of the experimental conditions needed to obtain multilayers from food-grade ingredients, and could represent a starting point for further applications in food products.

ACKNOWLEDMENTS

This research was supported by the Ministerio de Ciencia e Innovación (Spain) throughout projects ALG2009-11475. Author Acevedo-Fani also thanks to the University of Lleida for the pre-doctoral grant. Author Martín-Belloso acknowledges to the Institució Catalana de Recerca I Estudis Avançats (ICREA) for the Academia 2008 Award.

REFERENCES

(1) Guzey, D.; McClements, D. J. *Adv. Colloid Interface Sci.* **2006**, *128*, 227–248.

(2) Weiss, J.; Takhistov, P.; McClements, D. J.; Brunswick, N. *J. Food Sci.* **2006**, *71*, R107–R116.

(3) Fabra, M. J.; Busolo, M. A.; Lopez-Rubio, A.; Lagaron, J. M. *Trends Food Sci. Technol.* **2013**, *31*, 79–87.

(4) De Villiers, M. M.; Otto, D. P.; Strydom, S. J.; Lvov, Y. M. *Adv. Drug Deliv. Rev.* **2011**, *63*, 701–715.

(5) Decher, G. *Science.* **1997**, *277*, 1232–1237.

(6) Pawar, S. N.; Edgar, K. J. *Biomaterials* **2012**, *33*, 3279–3305.

(7) Lawrie, G.; Keen, I.; Drew, B.; Chandler-Temple, A.; Rintoul, L.; Fredericks, P.; Grøndahl, L. *Biomacromolecules* **2007**, *8*, 2533–2541.

(8) Sæther, H. V.; Holme, H. K.; Maurstad, G.; Smidsrød, O.; Stokke, B. T. *Carbohydr. Polym.* **2008**, *74*, 813–821.

(9) Klitzing, R. V. *Phys. Chem. Chem. Phys.* **2006**, *8*, 5012–5033.

(10) Alves, N. M.; Picart, C.; Mano, J. F. *Macromol. Biosci.* **2009**, *9*, 776–785.

(11) Yuan, W.; Dong, H.; Li, C. M.; Cui, X.; Yu, L.; Lu, Z.; Zhou, Q. *Langmuir* **2007**, *23*, 13046–13052.

(12) Caridade, S. G.; Monge, C.; Gilde, F.; Boudou, T.; Mano, J. F.; Picart, C. *Biomacromolecules* **2013**, *14*, 1653–1660.

(13) Lukomska, J.; Malicka, J.; Gryczynski, I.; Lakowicz, J. R. *J. Fluoresc.* **2004**, *14*, 417–423.

(14) Bech, L.; Meylheuc, T.; Lepoittevin, B.; Roger, P. *J. Polym. Sci. Part A Polym. Chem.* **2007**, *45*, 2172–2183.

(15) Irena, G.; Jolanta, B.; Karolina, Z. *Appl. Surf. Sci.* **2009**, *255*, 8293–8298.

(16) Choi, J.; Rubner, M. F. *Macromolecules* **2005**, *38*, 116–124.

(17) Lavalle, P.; Voegel, J.-C.; Vautier, D.; Senger, B.; Schaaf, P.; Ball, V. *Adv. Mater.* **2011**, *23*, 1191–1221.

(18) Shiratori, S. S.; Rubner, M. F. *Macromolecules* **2000**, *33*, 4213–4219.

(19) Vidyasagar, A.; Sung, C.; Losensky, K.; Lutkenhaus, J. L. *Macromolecules* **2012**, *45*, 9169–9176.

(20) Pargaonkar, N.; Lvov, Y. M.; Li, N.; Steenekamp, J. H.; de Villiers, M. M. *Pharm. Res.* **2005**, *22*, 826–835.

(21) Ai, H.; Jones, S. A.; de Villiers, M. M.; Lvov, Y. M. *J. Control. Release* **2003**, *86*, 59–68.

(22) Picart, C. *Curr. Med. Chem.* **2008**, *15*, 685–697.

(23) Crouzier, T.; Boudou, T.; Picart, C. *Curr. Opin. Colloid Interface Sci.* **2010**, *15*, 417–426.

(24) Xu, J.; Yang, L.; Hu, X.; Xu, S.; Wang, J.; Feng, S. *Soft Matter* **2015**, *11*, 1794–1799.

(25) Bieker, P.; Schönhoff, M. *Macromolecules* **2010**, *43*, 5052–5059.

(26) Kirby, B. J.; Hasselbrink, E. F. *Electrophoresis* **2004**, *25*, 203–213.

(27) Junka, K.; Sundman, O.; Salmi, J.; Osterberg, M.; Laine, J. *Carbohydr. Polym.* **2014**, *108*, 34–40.

(28) Schoeler, B.; Sharpe, S.; Hatton, T. A.; Caruso, F. *Langmuir* **2004**, *20*, 2730–2738.

(29) Salehi, A.; Desai, P. S.; Li, J.; Steele, C. A.; Larson, R. G. *Macromolecules* **2015**, *48*, 400–409.

(30) Richert, L.; Lavalle, P.; Payan, E.; Shu, X. Z.; Prestwich, G. D.; Stoltz, J.-F.; Schaaf, P.; Voegel, J.-C.; Picart, C. *Langmuir* **2004**, *20*, 448–458.

(31) Ladam, G.; Schaad, P.; Voegel, J. C.; Schaaf, P.; Decher, G.; Cuisinier, F. *Langmuir* **2000**, *16*, 1249–1255.

(32) Zhang, J.; Senger, B.; Vautier, D.; Picart, C.; Schaaf, P.; Voegel, J.-C.; Lavalle, P. *Biomaterials* **2005**, *26*, 3353–3361.

(33) Allen, K. W. Contact angle, wettability and adhesion. *International Journal of Adhesion and Adhesives*, 1994, *14*, 69.

(34) Kwok, D. Y.; Neumann, A. W. *Adv. Colloid Interface Sci.* **1999**, *81*, 167–249.

(35) Wu, T.; Sun, Y.; Li, N.; de Villiers, M. M.; Yu, L. *Langmuir* **2007**, *23*, 5148–5153.

(36) Almodóvar, J.; Place, L. W.; Gogolski, J.; Erickson, K.; Kipper, M. J. *Biomacromolecules* **2011**, *12*, 2755–2765.

(37) Fu, J.; Ji, J.; Yuan, W.; Shen, J. *Biomaterials* **2005**, *26*, 6684–6692.

(38) Yoo, D.; Shiratori, S. S.; Rubner, M. F. *Macromolecules* **1998**, *31*, 4309–4318.

(39) Deng, J.; Liu, X.; Ma, L.; Cheng, C.; Shi, W.; Nie, C.; Zhao, C. *ACS Appl. Mater. Interfaces* **2014**, *6*, 21603–21614.

(40) De Oliveira Santos, R. P.; Castro, D. O.; Ruvolo-Filho, A. C.; Frollini, E. *J. Appl. Polym. Sci.* **2014**, *131*, 40386.

(41) Grant, C. A.; Alfouzan, A.; Gough, T.; Twigg, P. C.; Coates, P. D. *Micron* **2013**, *44*, 174–178.

(42) Lee, C. S.; Yoon, K. H.; Park, J. C.; Kim, H.-U.; Park, Y.-B. *Fibers Polym.* **2014**, *15*, 1493–1499.

(43) Braun, D.; Cherdron, H.; Ritter, H. *Polymer Synthesis: Theory and Practice: Fundamentals, Methods, Experiments*; Springer Science & Business Media, 2013.

(44) Ayhan, Z.; Cimmino, S.; Esturk, O.; Duraccio, D.; Pezzuto, M.; Silvestre, C. *Packag. Technol. Sci.* **2015**, *28*, 589–602.

(45) Carneiro-da-Cunha, M. G.; Cerqueira, M. A.; Souza, B. W. S. S.; Carvalho, S.; Quintas, M. A. C. C.; Teixeira, J. A.; Vicente, A. A. *Carbohydr. Polym.* **2010**, *82*, 153–159.

TABLE OF CONTENTS GRAPHIC